Role of axonal sodium-channel band in neuronal excitability

Longfei Wang, Hengtong Wang, Lianchun Yu, and Yong Chen
Institute of Theoretical Physics, Lanzhou University, Lanzhou 730000, China
(Received 5 May 2011; published 2 November 2011)

Action potential initiation (API) is a crucial step in neural information integration and communication. A stable site of API is beneficial for neural coding. A specialized band with a high density of sodium channels in the axon initial segment has been proved as the primary site of API. In this paper we investigate the role of a dense sodium-channel band in the threshold and the location of API of a neuron with a multicompartment model. It is shown that the threshold of the injected current for API is enhanced by a farther distance between the stimulated site and the band and lowered by an increase of the sodium-channel density and the bandwidth. There exists an optimal location of the dense sodium-channel band, which enables the lowest threshold for API. In the case of an excitable dendrite, the site of API shifts from the band to the stimulated dendritic site with increasing stimuli strength. A larger bandwidth and higher sodium-channel density elevate the stability of the sodium-channel band as the site of API and an optimal band position enables the highest stability.

DOI: 10.1103/PhysRevE.84.052901 PACS number(s): 87.19.lb, 87.19.ll, 07.05.Tp

Action potential (AP) generation in neurons, in terms of action potential initiation (API), is an indispensable primary step of neuronal information processing. Action potential initiation is the key factor for every neuron to integrate thousands of synaptic inputs into the output signal, i.e., an all-or-none AP.

The site of API plays a significant role in stimulus thresholds [1], precise coding [2,3], and synaptic plasticity [4]. Early works have indicated that APs always initiate in the axon hillock or initial segment of an axon [5–7]. Recent evidence in a variety of neurons verified this classical notion and proved that APs are most often initiated at the distal end (30 μm farther) of the axon initial segment (AIS), i.e., the starting segment of axon [4,8–12]. The preference of API in the AIS is caused by the lowest voltage threshold resulting from a region with a higher density of the voltage-gated sodium (Na^+) channel than on dendrites and soma [4,9,10]. However, the dendritic APs are possible when the density of the sodium channel in dendrites is high enough for AP generation. Indeed, dendritic APs are observed in cortical CA1 pyramidal neurons [13], motoneurons [14], olfactory mitral cells [15], and hypothalamic gonadotropin-releasing hormone neurons [16]. In these cases, the sites of API shift from the somatoaxon region to dendrites, when the stimulus locations [16] (in dendrites) are distant from the somatic region and/or the stimulus strength is strong enough [15,17].

As the primary site of API, the dense Na^+ band plays an important role in regulating the neural excitability; however, it is still poorly known how the sodium-channel band works on regulating the neural activity. Until most recently, researchers showed that the location [18] and length [19] of the band can regulate the response of neurons to input signals. This is an impressive supplement for neuronal excitability and plasticity. As we know, the differences of sodium-channel bands widely exist in different cells [20]. Our work on the quantitative influence of the sodium band to neural excitability is significant to understand the variety of neural excitability and plasticity in different cells.

We employ a multicompartmental model [21] with Hodgkin-Huxley-style conductance [22] to study the neuronal API properties regulated by the dense sodium-channel band. As shown in Fig. 1, the modeled neuron is composed of a soma, a long nonbranching dendrite, and an unmyelinated nonbranching axon (designed according to the model used in Refs. [12,15,23]). The dendrite is directly attached to the soma, but the axon is connected to the soma with a tapered axon hillock. Uniform morphological and electrophysiological properties are used for the dendrite and axon except for the region of the dense sodium channel in the axon [4].

There are various density distributions of the sodium channel in the AIS such as uniform, decreasing, and increasing gradients [20] or with increasing peak from the soma and decreasing in the following distal axon [4,12,24], etc., for different cell types. In this work we use a uniform distribution of the sodium channel in the band. The uniform distribution is sufficient, in principle, to investigate the influence of the sodium-channel band on neural excitability.

Na^+-channel densities are denoted by the maximal Na^+-channel conductance $\bar{g}_{Na}$. We divide the densities of the Na^+ channel in different segments into three classes $\bar{g}^d_{Na}$, $\bar{g}^a_{Na}$, and $\bar{g}^b_{Na}$, reflecting the sodium-channel density of the dendrite, normal axon, and band, respectively (Fig. 1). The somatic density of the sodium channel is the same as the dendritic density. The dendritic and axonal densities are usually fixed, while $\bar{g}^b_{Na}$ is set by a ratio of H to the axonal sodium-channel density ($\bar{g}^b_{Na} = H\bar{g}^a_{Na}$). Note that there are two types of dendritic density: the normal weakly excitable dendrite ($\bar{g}^d_{Na} = 5\ mS/cm^2$) and the special fully excitable dendrite ($\bar{g}^d_{Na} = 50\ mS/cm^2$).

This model of nonbranching multicompartment neuron can be described by the following equations (modified from Ref. [22]):

$$c_m\frac{\partial V}{\partial t} = \frac{d(x)}{4R_a}\frac{\partial^2 V}{\partial x^2} - \bar{g}_{Na}(x)m^3h(V-E_{Na}) - \bar{g}_K n^4(V-E_K) - g_L(V-E_L) + i_e(t), \quad (1)$$

$$\frac{\partial m}{\partial t} = (1-m)\alpha_m(V) - m\beta_m(V), \quad (2)$$

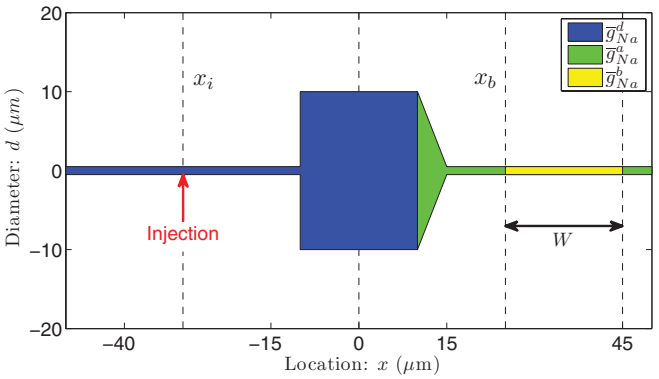

FIG. 1. (Color online) Schematic diagram of the neuron model. The morphology ratio between the radial and axial length scales is 1:1. Thin rectangles are the dendrite (left) and axon (right); the big rectangle (center) is the soma; the triangle is the axon hillock. Different colors show different densities of the sodium channel represented by sodium-channel conductance. Blue (dark, dendrite and soma), green (light, axon and axon hillock), and yellow (blank, the sodium band, middle of the axon in the figure) represent the sodium-channel conductance of $\bar{g}^d_{\rm Na}$, $\bar{g}^a_{\rm Na}$, and $\bar{g}^b_{\rm Na}$. The injected location of the external current injection and the starting position of the sodium-channel band are denoted by x_i and x_b, respectively and the bandwidth is denoted by W.

$$\frac{\partial n}{\partial t} = (1-n)\alpha_n(V) - n\beta_n(V), \tag{3}$$

$$\frac{\partial h}{\partial t} = (1-h)\alpha_h(V) - h\beta_h(V), \tag{4}$$

where V is an abbreviation for the membrane potential $V(x,t)$ and m, n, and h are shortened terms for the activation variables $m(x,t)$, $n(x,t)$, and $h(x,t)$, respectively. The leak current g_L is a constant for all the compartments. Sodium- (potassium-) channel densities are represented by maximal ion-channel conductances $\bar{g}_{\rm Na}$ ($\bar{g}_{\rm K}$). A typical set of voltage-dependent gating functions $\alpha(V)$ and $\beta(V)$ are used [22], $\alpha_m = 0.1\frac{25-V}{e^{(25-V)/10}-1}$, $\beta_m = 4.0e^{-V/18}$, $\alpha_n = 0.01\frac{10-V}{e^{(10-V)/10}-1}$, $\beta_n = 0.125e^{-V/80}$, $\alpha_h = 0.07e^{-V/20}$, and $\beta_h = \frac{1}{e^{(30-V)/10}+1}$. The external current injection i_e is the synapticlike current by default: $i_e(t) = I_e\,(t-t_i)\,e^{-(t-t_i)/\tau}$ for $t \geqslant t_i$ and 0 for $t < t_i$. The current is added to one segment in all simulations; $t_i = 30$ ms ensures that the whole neuron is in the resting state before current injection. The parameter τ, which reflects the duration of stimulus pulse, is set equal to 5 ms. (For a list of the parameters in all the simulations, see Table I.)

When and where the AP initiates (the time and site of the API) are determined empirically by the time and location at which the first segment reaches a threshold voltage 50 mV. However, in simulations, the maximal potential of the whole neuron must reach 80 mV and the minimal potential must be less than −15 mV to confirm the increase of the AP in our neuron model.

As displayed in Fig. 2, we use I_e to denote the amplitude of the synapticlike current. When $I_e < I_{\rm th}$, no AP could be triggered. Conversely, the input current always induces an AP, no matter where the AP is initiated. This is consistent with the all-or-none property of the AP. If I_e crosses $I_{\rm th} + \Delta I$, the site of the API will shift with the current amplitude from the AIS to the stimulated region, when the dendrite is fully excitable.

TABLE I. Default values of morphological and biophysical parameters in all simulations.

Parameter	Symbol	Value	Units
axonal or dendritic diameter	d_a, d_d	1.0	μm
somatic diameter	d_s	20.0	μm
membrane capacitivity	C^a_m, C^d_m, C^s_m	1.0	μF/cm^2
axial or intracellular resistivity	R_a	35.4	Ω cm
leakage reversal potential	E_L	11.0	mV
K^+ reversal potential	$E_{\rm K}$	−12.0	mV
Na^+ reversal potential	$E_{\rm Na}$	115.0	mV
leakage conductance	g_L	0.3	mS cm^{-2}
K^+ conductance	$\bar{g}_{\rm K}$	86.0	mS cm^{-2}
dendritic Na^+ conductance	$\bar{g}^d_{\rm Na}$	5.0/50.0	mS cm^{-2}
axonal Na^+ conductance	$\bar{g}^a_{\rm Na}$	50.0	mS cm^{-2}
Na^+ conductance in the band	$\bar{g}^b_{\rm Na} = H\bar{g}^a_{\rm Na}$	10×50.0	mS cm^{-2}

Note that ΔI describes the range of the input-current amplitude for successfully generating an AP at the dense sodium band. A larger ΔI reflects that the band is a more stable site for API; $\Delta I = 0$ means that the site of API is always near the stimulated segment and corresponds to the dendrite being the primary site of API [16].

We calculate $I_{\rm th}$ and ΔI for x_b, W, and H (the start position, the width of the band, and the ratio of densities in the band and normal axon) changing under a few different stimulation sites ($x_i = -20$, -40, -60, -80, -100, and -120 μm) to get relatively complete response properties of the neuron and investigate the role of the band on neuronal excitability. We first show the results for the model neuron with a weakly excitable dendrite. Dendrites usually have only a low-density Na^+-channel band to enable backpropagating APs and APs always initiate at the axon and backpropagate to the soma and dendrites in most neurons [25,26].

In Fig. 3(a) the current threshold $I_{\rm th}$ increases with increasing distance between the band and soma (x_b), which indicates that, for a band farther away, stronger currents are

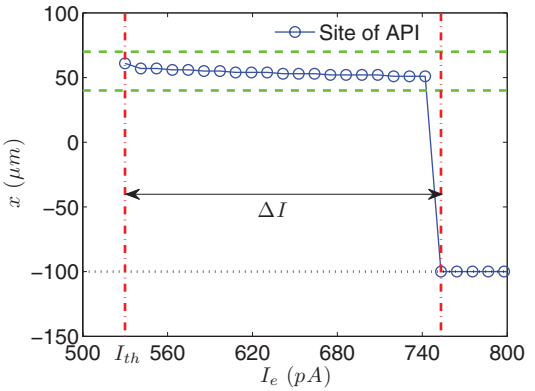

FIG. 2. (Color online) The site of API changes with increasing amplitude of input synaptic currents. The left red dash-dotted line indicates the current threshold $I_{\rm th}$, while the right one shows the shift of APIs from the dense sodium-channel band to the site of the injecting current; ΔI denotes the current range of APIs on the band. The horizontal green dashed lines depict the band location. The black dotted line denotes the injection site. Here $x_i = -100$ μm, $x_b = 40$ μm, $W = 30$ μm, $\bar{g}^d_{\rm Na} = 50$ mS/cm^{-2}.

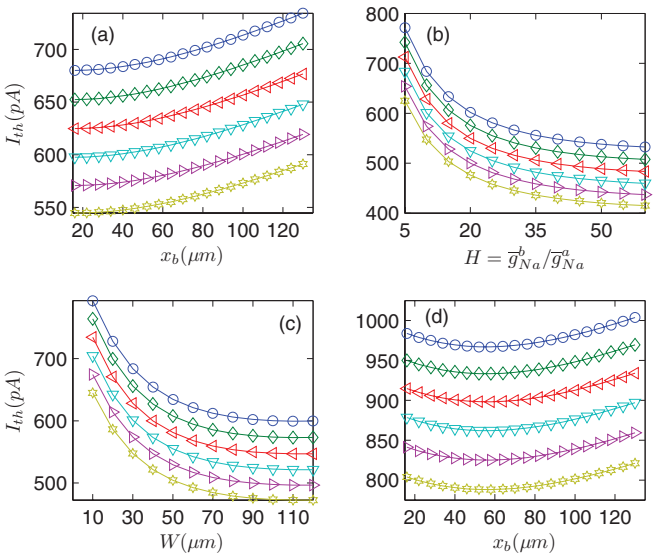

FIG. 3. (Color online) The current threshold I_{th} varies with (a) the band position x_b, (b) the density ratio of the sodium channel H, (c) the bandwidth W, and (d) the band position x_b. Lines with different colors and markers correspond to different injection locations: yellow hexagrams, magenta right-oriented triangles, cyan down-oriented triangles, red left-oriented triangles, green diamonds, and blue circles are $x_i = -20$, -40, -60, -80, -100, and -120 μm, respectively. All parameters are default values except for the somatic diameter of 40 μm in (d).

required to trigger APs. The lower-threshold region caused by the band shifts farther and stronger currents are needed to make the attenuated fluctuation of the membrane potential propagate more distally to excite APs. Figure 3(b) plots the threshold properties for different Na^+-channel density ratios of the band to the normal axon. With increasing density ratio or bandwidth, I_{th} decreases quickly for all the injection sites and then becomes stable with further increases. The higher the density ratio or the wider the bandwidth is, the easier the neuron generates an AP. Similarly, the increase of bandwidth also lowers the threshold I_{th} for all the injection sites [see Fig. 3(c)]. The lowering effect of the bandwidth comes from the coupling effects between neighborhood segments. The band segments not only reduce their thresholds but also decrease the thresholds of nearby sites.

The monotonic growth of the threshold with a more distant sodium-channel band (increasing x_b) indicates that the band should be as close as possible to the soma to enhance the neural excitability. However, the biophysical evidence shows that the band normally is not located at the soma, the axon hillock, or the start of the axon, but settles on the distal end of the AIS [4,9,10]. The most probable explanation is the great influence of the soma on nearby parts. The soma is large and many attached dendrites, thus the membrane potentials of the soma and the nearby parts are hard to change. In our simulations, the size of the soma is controlled by the diameter, length, and number of somatic segments, while the influence of the attached dendrites can be realized by enlarging the membrane capacity of the soma. With a large soma [diameter 40 μm; see Fig. 3(d)], the thresholds decrease first and then increase with a minimal value. If the band is closer to the soma the threshold may increase. This phenomenon has been observed by comparing the higher-voltage threshold in dentate granule neurons, which have a proximal axon sodium-channel distribution, with CA3 pyramidal neurons [1]. The minimal threshold implies an optimal distance between the soma and the band.

Though weakly excitable dendrites and axonal APs are common, dendritic APs (or spikes) are also observed in serval neuron types [13–16]. They can be easily inspired when a neuron has a high dendritic density of Na^+ channels [14,15]. Thus we investigate the excitability regulation in a neuron with a fully excitable dendrite whose sodium-channel densities are enough to generate APs.

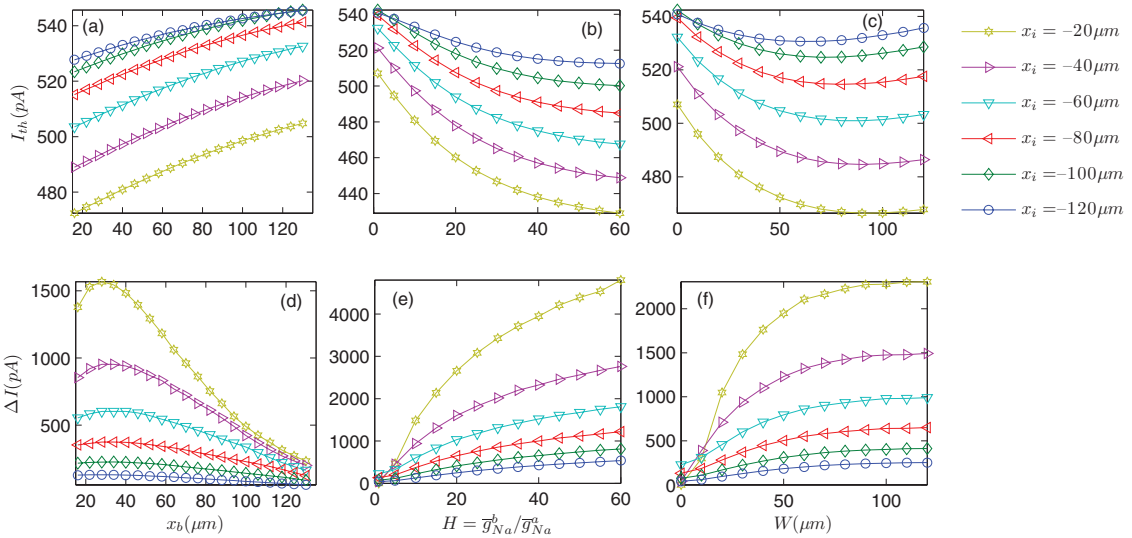

FIG. 4. (Color online) Regulation of the threshold by the sodium-channel band in the neuron with a fully excitable dendrite. The current threshold I_{th} varies with (a) the band position x_b, (b) the sodium-channel density ratio H, and (c) the bandwidth W. The current range ΔI corresponds to (d) the band location x_b, (e) the density ratio H, and (f) the bandwidth W. Here the dendrite is fully excitable ($g^d_{\text{Na}} = 50$ mS/cm^2) and the other parameters are the default values.

Compared with a neuron with a weakly excitable dendrite, the neuron with a fully excitable dendrite exhibits similar behavior in the threshold regulation by the sodium-channel band (see Figs. 3 and 4). When the band is located closer to the soma, the threshold is lower [Fig. 4(a)]. The increases of the channel density and bandwidth reduce thresholds too [Figs. 4(b) and 4(c)]. The thresholds are all lower than the neuron with a weakly excitable dendrite.

The scale of the AP initiated near the band in the AIS is denoted by ΔI. A larger ΔI implies that the band is the more stable site of API under a larger scale of external inputs. Thus the largest value of ΔI, as displayed in Fig. 4(d), suggests that the neuron has a more stable site of API compared with the band located at other positions, which indicates that there is an optimal band location. When the band is too far from the soma, ΔI declines toward zero and APs are more likely to be initiated at the stimulated site in the dendrites rather than the band in the AIS. Figure 4(e) exhibits the regulation of sites of API by the density ratio H. Higher densities of the Na^+ channel (larger H) make the band a more stable site of API. Figure 4(f) shows that the preference of the AIS in API is also enhanced by expanding the distal end of the bands.

In summary, based on fine-resolution simulations with a bipolar neuron, we studied the influence of the sodium-channel band on neuronal excitation, including the current threshold and the reliability of API in the AIS. In the case of weakly excitable dendrites, it is found that the current threshold decreases with increasing density of the Na^+ channel and the bandwidth. The farther band location enlarges the threshold and a location near the soma has the lowest threshold. With increasing height and width of the band, the current threshold decreases to saturation. The threshold regulation in the neuron with fully excitable dendrites is similar to that with weakly excitable dendrites.

Our results are consistent with recent experiments. The regulation of neuronal excitability by changing the properties of the sodium-channel band does indeed exist and neural excitability is regulated in the same way as shown by our results. Grubb and Burrone found that the distal shift of the band significantly increases in the threshold current and the threshold current density for firing an AP and thus reduces the neural excitability in hippocampal neurons during development [19]. The effect of relocation of the sodium band to neural excitability is consistent with our conclusion of a negative relationship of the current threshold and start position of the band from the soma (I_{th} vs x_b). In our results, the increase in bandwidth can lower the current threshold of a neuron, which is confirmed by Kuba *et al*. [18]. They showed that the length of the initial segment labeling with voltage-gated Na^+ channels increases by 1.7 times in 7 days after auditory input deprivation and the elongation of the sodium band enhanced the neural excitability: The threshold potential decreased by 4 mV and the threshold current was reduced by 30% [18].

The distribution of the sodium-channel band in the AIS is a crucial factor of neural excitability. The various distributions of the sodium channel at the band on different neurons result in a variety of neural excitabilities. Though the present work is limited to single API and nonbranching neurons with an unmyelinated axon, our results exhibit, in principle, the quantitative influences of the sodium-channel band on neural excitability. In contrast, the neural activity is able to adjust the properties of the sodium-channel band in neural development [18,19]. The correlation between of neuronal electrical activity and the sodium-channel band is worth further intensive exploration.

This work was supported by the National Natural Science Foundation of China (Grants No. 10975063 and No. 11105062) and the Fundamental Research Funds for the Central Universities of Lanzhou University (Grant No. lzujbky-2011-57).

[1] G. J. Kress, M. J. Dowling, L. N. Eisenman, and S. Mennerick, Hippocampus **20**, 558 (2010).
[2] H. Kuba, T. M. Ishii, and H. Ohmori, Nature (London) **444**, 1069 (2006).
[3] H. Kuba and H. Ohmori, J. Physiol. **587**, 87 (2009).
[4] W. Q. Hu *et al*., Nature Neurosci. **12**, 996 (2009).
[5] J. S. Coombs, D. R. Curtis, and J. C. Eccles, J. Physiol. (London) **139**, 232 (1957).
[6] J. S. Coombs, D. R. Curtis, and J. C. Eccles, J. Physiol. (London) **139**, 198 (1957).
[7] M. G. F. Fuortes, K. Frank, and M. C. Becker, J. Gen. Physiol. **40**, 735 (1957).
[8] A. Foust, M. Popovic, D. Zecevic, and D. A. McCormick, J. Neurosci. **30**, 6891 (2010).
[9] M. H. P. Kole *et al*., Nature Neurosci. **11**, 178 (2008).
[10] S. I. Fried *et al*., J. Neurophysiol. **101**, 1972 (2009).
[11] L. M. Palmer and G. J. Stuart, J. Neurosci. **26**, 1854 (2006).
[12] J. P. Meeks and S. Mennerick, J. Neurophysiol. **97**, 3460 (2007).
[13] S. Gasparini, M. Migliore, and J. C. Magee, J. Neurosci. **24**, 11046 (2004).
[14] H.-R. Lüscher and M. E. Larkum, J. Neurophysiol. **80**, 715 (1998).
[15] G. Y. Shen *et al*., J. Neurophysiol. **82**, 3006 (1999).
[16] C. B. Roberts, R. E. Campbell, A. E. Herbison, and K. J. Suter, Endocrinology **149**, 3355 (2008).
[17] W. R. Chen *et al*., J. Neurophysiol. **88**, 2755 (2002).
[18] H. Kuba, Y. Oichi, and H. Ohmori, Nature (London) **465**, 1075 (2010).
[19] M. S. Grubb and J. Burrone, Nature (London) **465**, 1070 (2010).
[20] A. Lorincz and Z. Nusser, J. Neurosci. **28**, 14329 (2008).
[21] P. Dayan and L. F. Abbott, *Theoretical Neuroscience: Computational and Mathematical Modeling of Neural Systems* (MIT Press, Cambridge, MA, 2001).
[22] A. L. Hodgkin and A. F. Huxley, J. Physiol. (London) **117**, 500 (1952).
[23] S. Zeng and Y. Tang, Phys. Rev. E **80**, 021917 (2009).
[24] C. Schmidt-Hieber and J. Bischofberger, J. Neurosci. **30**, 10233 (2010).
[25] M. Rapp, Y. Yarom, and I. Segev, Proc. Natl. Acad. Sci. USA **93**, 11985 (1996).
[26] Y. Shu, A. Duque, Y. Yu, B. Haider, and D. A. Mccormick, J. Neurophysiol. **97**, 746 (2007).